DAMAGE IDENTIFICATION IN A FULL-SCALE BRIDGE STRUCTURE

Wirtu L. Bayissa[1*] and Nicholas Haritos[2]

[1]PhD student in Civil Engineering, The University of Melbourne, Victoria 3010, Australia
*E-mail: w.bayissa@civenv.unimelb.edu.au, wrtlem@yahoo.com

[2]Assoc. Professor and Reader in Civil Engineering, The University of Melbourne, Australia

ABSTRACT

In this paper, the significance of vibration-based structural damage localization parameters that can be employed after the structure is subjected to fatigue cracking or after the occurrence of extreme events such as earthquakes and blast loads is demonstrated on "real-world" experimental data obtained from a full-scale bridge structure. First, "damage-sensitive" response parameters determined in the time/spectral domain, wavelet domain and modal domain are presented for damage localization in the context of a non model-based damage identification approach. Consequently, experimental modal data (namely resonance frequencies, mode shapes and modal damping) obtained from US Interstate Highway 40 (I-40) Bridge subjected to various damage conditions is employed for localization of damage in the plate girder of the bridge. The results obtained demonstrate the robustness and relevance of vibration-based methods for localization of damage in a full-scale structure in the presence of sparse modal information and incomplete measurement grid points. Finally, the proposed methods can be applied to input-output as well as output-only damage identification problems.

Keywords: Damage localization; power spectral density; wavelets; statistical moments; bridge

1. INTRODUCTION

In the past, vibration-based techniques have been widely used for damage identification and health monitoring in the areas of aerospace, automotive, civil and mechanical engineering (Doebling, 1996). Various vibration-based response parameters have been employed for localization of structural damage after the structure is subjected to fatigue cracking or after the occurrence of extreme events such as earthquakes and blast loads. These include *resonance frequency* based methods (natural frequency (Cawley and Adams, 1979), modal flexibility and its derivatives (Zhang and Aktan, 1998), modal strain energy (Cornwell et al., 1999)); *broadband frequency* based methods (frequency response functions (Sampaio et al, 1999), response power spectral density based methods (Bayissa and Haritos, 2007), spectral strain energy (Bayissa and Haritos, 2007), wavelet analysis based methods (Yam et al., 2003)). However, the majority of these methods are often employed either in a

simulation environment or on experimental data from simple structures. Therefore, the focus of this paper is to demonstrate the robustness of the *broadband frequency* based damage identification parameters, namely the mean square value (MSV), spectral strain energy (SSE) and zeroth-order moment (ZOM) of wavelet power spectra using experimental data from a full-scale bridge known as I-40 bridge. The reader may refer to Farrar, et al. (1994) and Farrar and Jauregui (1998) for extensive damage localization studies conducted on the I-40 Bridge using five *resonance frequency* based methods.

2. DESCRIPTION OF THE I-40 BRIDGE

The US Interstate Highway 40 (I-40) Bridge in New Mexico is made up of a concrete deck supported by two welded-steel and cross-braced plate girders, three steel stringers supported by a system of floor beams, and steel plate girders supported by concrete abutments and/or piers. The bridge comprises of three independent and identical sections where each section contains three spans. The elevation view of the portion of the I-40 Bridge used for the modal testing, analysis and damage identification studies is shown in Fig. 1(a). The damage scenarios induced to the bridge were intended to simulate the formation of a fatigue crack that may occur in plate-girder bridges under field conditions. As a result, various damage scenarios were introduced at a single location to the middle span of the north plate girder of the bridge. The damage scenarios considered in this study include: (i) damage scenario E-3: which consisted of an 183 cm long cut in the web extending halfway into the bottom flange towards either side; (ii) damage scenario E-4: consisting of this 183 cm long cut in the web extending through the entire bottom flange.

2.1 Data Acquisition and Analysis

Two types of vibration tests were conducted on the I-40 Bridge: forced vibration tests (FVTs) and ambient vibration tests (AVTs). The FVTs were conducted on the portion of the I-40 Bridge using 26 accelerometers mounted on the two plate girders. Hence, the number of accelerometers used on the north plate girder where damage was induced was 13 (Fig. 1(b)). The measurement data set obtained from this test was referred in the referenced literature as SET1 (Farrar, et al., 1994; Farrar and Jauregui, 1998). The modal parameters for various damage condition states were extracted from the FRFs and the mode shapes were *unit-mass* normalized prior to the computation of the damage identification parameters. Similarly, AVT was conducted using 11 accelerometers on the middle span of the north plate girder of the bridge portion tested using random input excitation from a shaker (Fig. 2). The measurement data set obtained from this test is referred to as SET2. Consequently, the modal parameters were extracted from the amplitude and phase information of the cross-power spectra of the acceleration responses (Farrar, et al., 1994). The mode shapes obtained were then normalized using an *identity mass* matrix.

Finally, modal data obtained from FVT were used for input-output damage identification while those obtained from AVT were employed for output-only damage identification. Moreover, for all the damage localization studies conducted, modal parameters of the first 2 modes were employed. A cubic spline interpolation was applied to determine mode shapes at a refined set of grid points. The normalized DI was used for localization of damage.

3. DAMAGE LOCALIZATION PARAMETERS

3.1 The Mean Square Value

In the past, the mean square value (MSV) of the vibration response signal, which can be determined either in the time-domain or spectral domain, has been identified to be sensitive to local and global damage with significant advantages over commonly adopted non model-based damage identification methods (Bayissa and Haritos, 2005), given by:

(a) Time domain:

$$\text{MSV} = \frac{1}{T}\int_0^{T_s} |y(t)|^2 dt \equiv \frac{1}{N}\sum_{n=0}^{N-1} |y[t_n]|^2 \tag{1}$$

where $y(t)$ denotes the vibration response signal; $y[t_n]$ is an N point sequence of $y(t)$; and T is the sampling length.

(b) Spectral/Frequency domain:

$$\text{MSV} = \frac{1}{2\pi}\int_{-\infty}^{\infty} S_{yy}(\omega) d\omega \equiv \frac{1}{2\pi}\int_{-\infty}^{\infty} |H(\omega)|^2 S_{pp}(\omega)\, d\omega \tag{2}$$

where $S_{yy}(\omega)$ is a two-sided response PSD; $H(\omega)$ denotes the FRF; $S_{pp}(\omega)$ is the excitation PSD; and ω is the excitation frequency.

(c) Modal domain:

$$\text{MSV} = \frac{1}{2\pi}[\phi][\phi]^T \int_{-\infty}^{\infty} [H_r^*(\omega)][S_{pp}(\omega)][H_r(\omega)] d\omega\, [\phi]^T[\phi] \tag{3}$$

where $H_r(\omega)$ is the diagonal matrix of the modal FRF, $H_r^*(\omega)$ is the complex conjugate of $H_r(\omega)$. For a beam-like structure, the MSV at a grid point k due to lateral random excitation at a grid point l is obtained from Eq. (2), ignoring the cross-spectral terms, as:

$$\text{MSV} \approx \frac{1}{2\pi}\int_{-\infty}^{\infty}\left(\sum_{r=1}^{\infty} \frac{\left(\phi_r^k\right)^2\left(\phi_r^l\right)^2}{\left(\omega_r^2 - \omega^2\right)^2 + \left(2\zeta_r\omega_r\omega\right)^2}\right) S_{pp}(\omega)\, d\omega \tag{4}$$

where ϕ_r^k is the r^{th} mass-normalized mode shape vector at grid point k, ϕ_r^l the corresponding mass-normalized mode shape vector at grid point l. ω_r and ζ_r are the natural frequency and the damping ratio of the r^{th} mode, respectively.

3.2 The Spectral Strain Energy

The spectral strain energy (SSE) used for the damage localization is given by (Bayissa and Haritos, 2007):

$$\text{SSE} = \left(\frac{EI}{2\pi}\right)^2 \int_0^L \int_{-\infty}^{\infty} \left\{ \sum_{r=1}^{\infty} \frac{\left(\frac{\partial^2\phi_r^k}{\partial x^2}\right)^2 \left(\frac{\partial^2\phi_r^k}{\partial x^2}\right)^2 \left(\phi_r^l\right)^4}{\left(\left(\omega_r^2 - \omega^2\right)^2 + \left(2\zeta_r\omega_r\omega\right)^2\right)^2} \right\} S_{pp}^2(l,\omega)\, d\omega\, dx \tag{5}$$

where EI is the bending rigidity, in which E is the Young's modulus and I is the moment of inertia. L is the span length of the beam-like structure.

3.3 Zeroth-Order Moment of the Wavelet Power Spectra

The zeroth-order moment (ZOM) of the joint time-frequency density function of the signal employed for damage localization in the I-40 Bridge is given by:

$$(\mu^0)_{t,f} = E[C(t,f)] = \int_{-\infty}^{\infty}\int_{-\infty}^{\infty} C(t,f)\,dt\,df \tag{6}$$

where $(\mu^0)_{t,f}$ denotes the ZOM; $C(t,f)$ is the joint energy density function; t and f are time and frequency, respectively; and $E[.]$ is an expectation operator. $C(t,f)$ can be determined in terms of wavelet power spectra, as follows (Torrence and Compo, 1998):

$$C(t,f) = \left|Q(\alpha,\beta)\right|^2 \tag{7}$$

where $Q(\alpha,\beta)$ contains the coefficients of the continuous wavelet transform(CWT); α and β are the scale and translation parameters, respectively.

4. DAMAGE LOCALIZATION INDEX

4.1 Normalized Damage Index (NDI)

In this study, the concept of statistical hypothesis testing is adopted to localize damage based on pre-defined damage threshold values. Moreover, division by the norm of the damage identification parameters and shifting of the reference coordinate by 1 were conducted prior to computation of the element-based damage index (DI^e), as follow:

$$\mathrm{DI}^e = \frac{\left[\dfrac{\int_{dL}\left(RP^{De}\right)dx}{\left\|\left\{\int_{dL}\left(RP^{De}\right)dx\right\}\right\|}\Big/\dfrac{1}{ne}\sum_{e=1}^{ne}\dfrac{\int_{dL}\left(RP^{De}\right)dx}{\left\|\left\{\int_{dL}\left(RP^{De}\right)dx\right\}\right\|}\right]+1}{\left[\dfrac{\int_{dL}\left(RP^{Ue}\right)dx}{\left\|\left\{\int_{dL}\left(RP^{Ue}\right)dx\right\}\right\|}\Big/\dfrac{1}{ne}\sum_{e=1}^{ne}\dfrac{\int_{dL}\left(RP^{Ue}\right)dx}{\left\|\left\{\int_{dL}\left(RP^{Ue}\right)dx\right\}\right\|}\right]+1} \tag{8}$$

where RP^{Ue} and RP^{De} are the undamaged and damaged response parameters (i.e., MSV, SSE and ZOM) for element e, respectively; ne is the number of elements considered for the damage localization process; dL is the length of each element e. Moreover, DI^e is standardized prior to the application of hypothesis testing, as follows:

$$\mathrm{Z}^e = \frac{\mathrm{DI}^e - \mu_{DI}}{\sigma_{DI}} \tag{9}$$

where μ_{DI}, σ_{DI} are the mean and standard deviation of DI^e. Assuming that Z^e is a normally distributed random variable, localization of damage can be conducted using a one-tailed hypothesis test, as: (i) choose H_0 (element e is not damaged) if $\mathrm{Z}^e < C_r$, or (ii) choose H_1 (element e is damaged) if $\mathrm{Z}^e \geq C_r$, where C_r the threshold value. Typical C_r values widely used in the literature include 1.28, 2 and 3 for 90%, 95% and 99% confidence levels, respectively.

4.2. Damage Localization Results

(1) Damage Localization Results from the MSV Method: Damage localization results obtained from the MSV method in terms of normalized DI are presented in Figs. 3.1(a)–(b) and 3.2(a)–(b) for SET1 and SET2 measurement data, respectively. In both cases, the normalized DI was found to effectively localize damage scenarios E-3 and E-4 (Fig. 3.1(a)–(b) and 3.2(a)–(b)). Therefore, these results demonstrate that the MSV parameter is robust and reliable for damage identification in real structure.

(2) Damage Localization results from the SSE Method: Damage localization results of the normalized SSE method are presented in Figs. 4.1(a)–(b) and 4.2(a)–(b) for SET1 and SET2 data, respectively. From the observation of the values of the normalized DI greater or equal to 2, it can be concluded that SSE is able to localize both damage scenario E-3 and E-4 using coarse (SET1) as well as refined (SET2) measurement data. For damage scenario E-3, minor SSE responses were observed at locations other than the actual damage location, (see Figs. 4.1(a) and 4.2(a)).

(3) Damage Localization results from the ZOM Method: In this section, damage localization results of the ZOM method in terms of normalized damage DI are presented in Figs. 5.1(a)–(b) and 5.2(a)–(b) for SET1 and SET2 data, respectively. As can be observed, the normalized DI was able to effectively localize both damage scenarios E-3 and E-4 accurately for both SET1 and SET2 measurement data. These results show that the ZOM is an effective response parameter to localize the damage in a full-scale bridge using input-output as well as output-only experimental modal data.

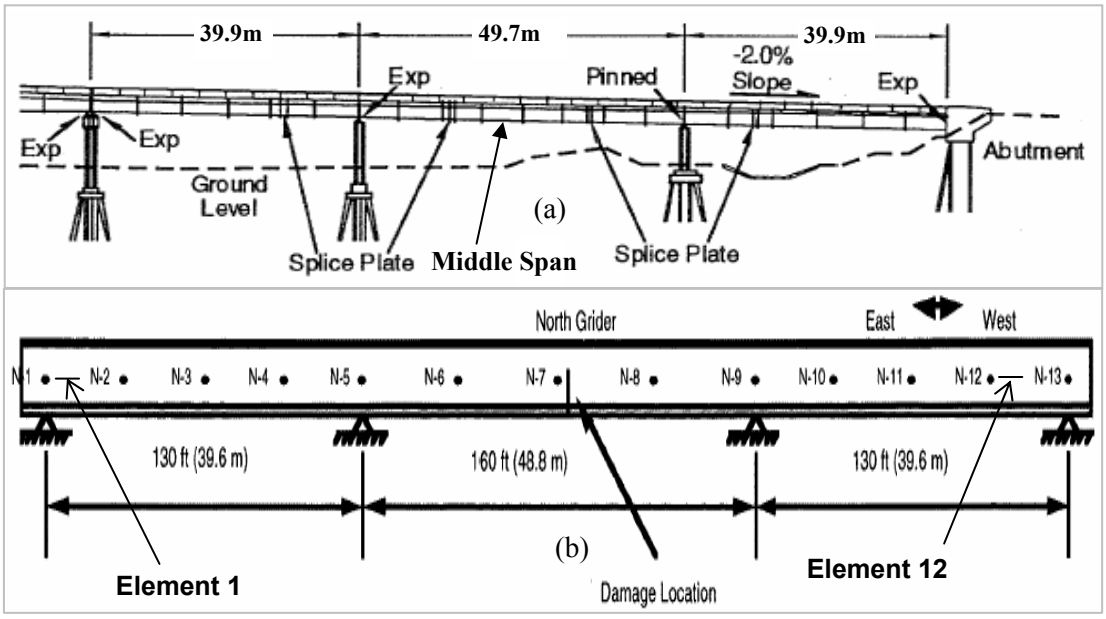

Fig. 1. Locations of the SET1 accelerometers during the FVTs: (a) portion of the I-40 Bridge tested; (b) north plate girder with location of damage and accelerometers indicated.

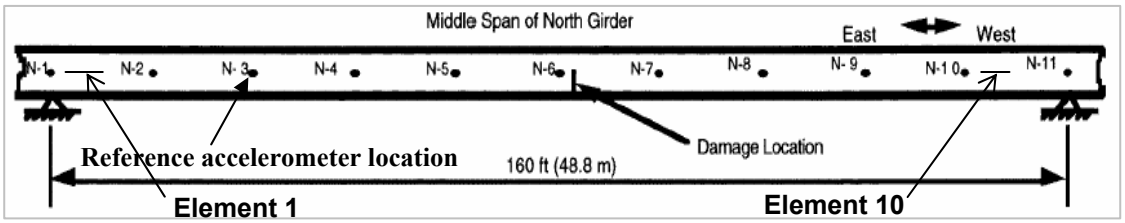

Fig. 2. Location of SET2 accelerometers on the middle span of the north plate girder during AVTs of the I-40 Bridge.

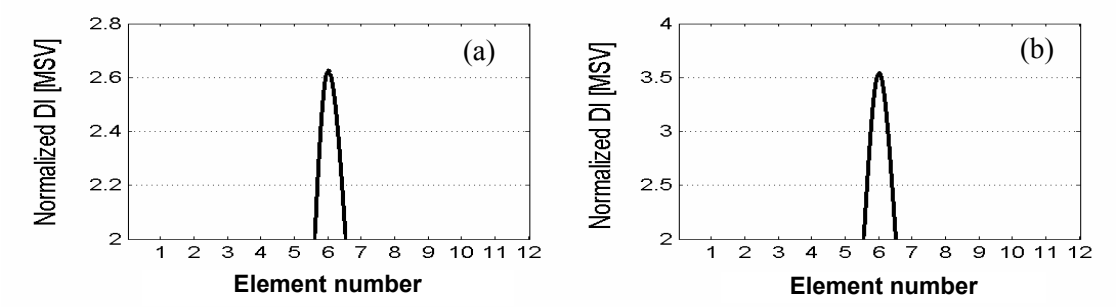

Fig. 3.1 Damage identification results from normalized MSV of response of the I-40 Bridge using SET1 modal data: (a) damage scenario E-3; (b) damage scenario E-4.

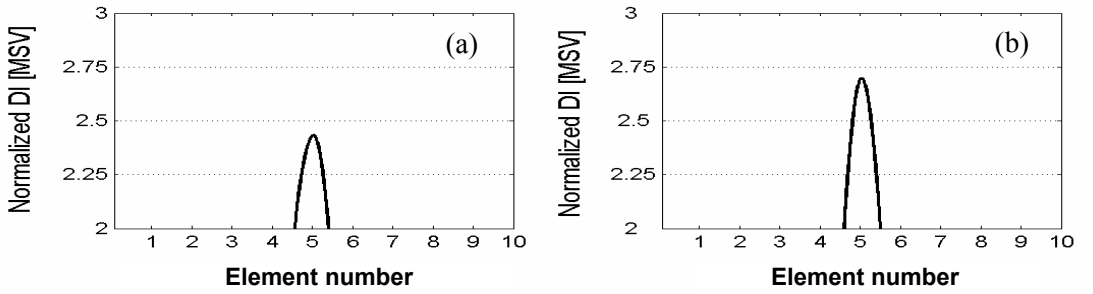

Fig. 3.2 Damage identification results from normalized MSV of response of the I-40 Bridge using SET2 modal data: (a) damage scenario E-3; (b) damage scenario E-4.

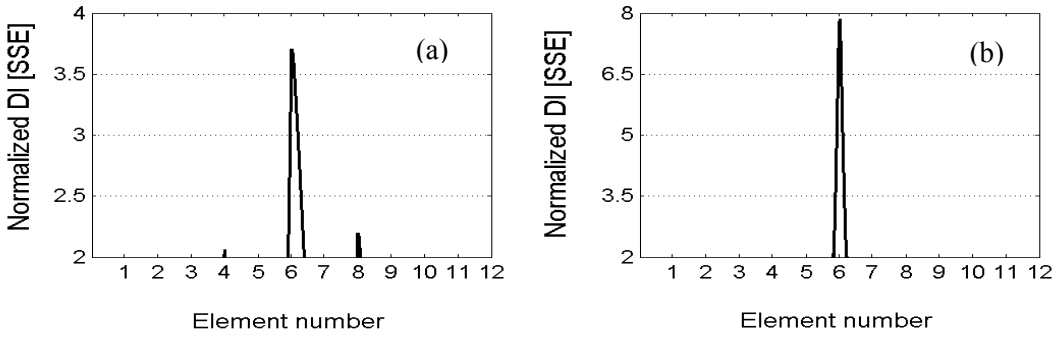

Fig. 4.1. Damage localization results from normalized response SSEs of the I-40 Bridge using SET1 modal data: (a) damage scenario E-3; (b) damage scenario E-4.

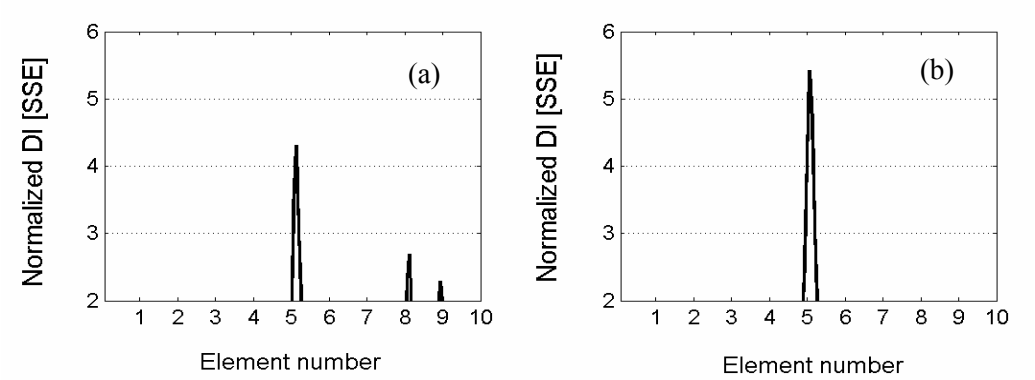

Fig. 4.2. Damage localization results from normalized response SSEs of the I-40 Bridge using SET2 modal data: (a) damage scenario E-3; (b) damage scenario E-4.

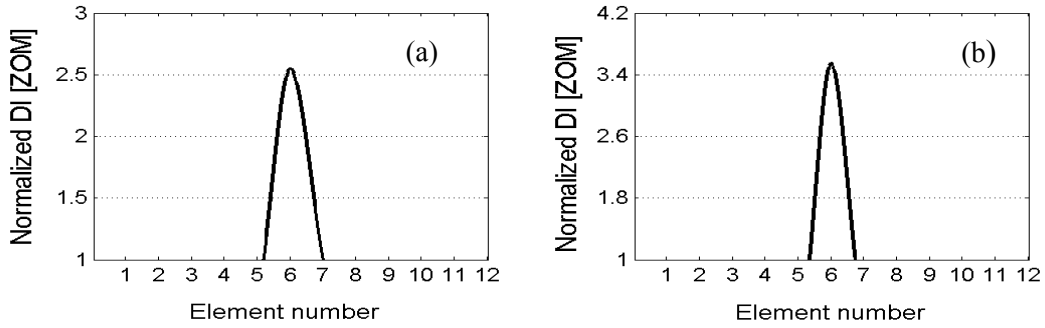

Fig. 5.1. Damage localization results from normalized ZOM of the wavelet spectra using SET1 data: (a) damage scenario E-3; (b) damage scenario E-4.

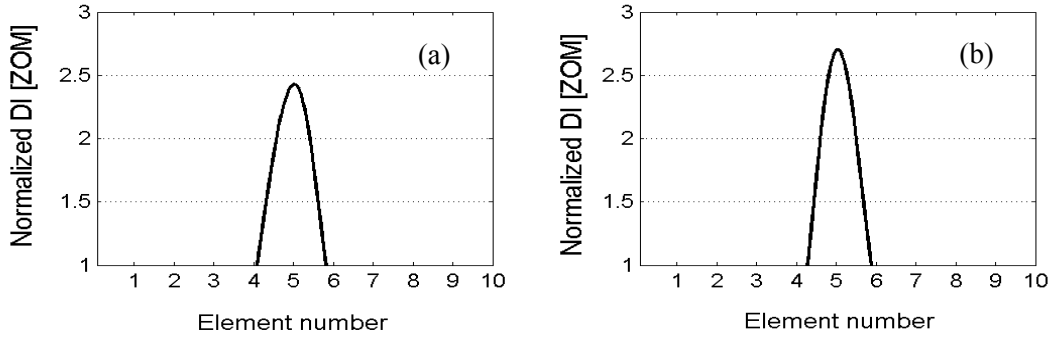

Fig. 5.2. Damage localization results from normalized ZOM of the wavelet spectra using SET2 data: (a) damage scenario E-3; (b) damage scenario E-4.

5. CONCLUSIONS

The experimental verification studies presented in this paper illustrate the robustness of the vibration-based structural damage identification tools for monitoring and diagnostic

condition assessment of real-life infrastructure subjected to fatigue cracking or after the occurrence of extreme events such as earthquakes and blast loads. The improved capability of the *broadband frequency* based damage localization methods has been demonstrated with real vibration response data from a full-scale structure in the presence of sparse modal information, measurement data from a limited number of measurement grid points and uncontrolled random excitation. Moreover, comparisons of the results with those reported in the literature using existing *resonance frequency* based methods and the same standard set of experimental data highlight the robustness and superior performance of the *broadband frequency* based parameters for damage localization in a "real-world" application.

REFERENCES

Bayissa, W.L. and Haritos, N. (2005) Structural damage assessment using the mean square value of response power spectral density, Proceedings of Australian Structural Engineering Conference, Sept. 11-14, Newcastle, Australia, No 27, CD-ROM.

Bayissa, W.L. and Haritos, N. (2007) Damage identification in plate-like structures using spectral strain energy analysis, Journal of Sound and Vibration Vol 307, pp 226-229.

Cawley, P. and Adams, R.D. (1979) The location of defects in structures from measurements of natural frequencies, Journal of Strain Analysis for Engineering Design Vol 14, pp 49–57.

Cornwell, P. Doebling, S.W. and Farrar, C.R. (1999) Application of the strain energy damage detection method to plate-like structures, Journal of Sound and Vibration Vol 224, pp 359–374.

Doebling, S.W., Farrar, C.L., Prime, M.B. and Shevitz, D.W. (1996) Damage identification and health monitoring of structural and mechanical systems from changes in their vibration characteristics: A literature review, Los Alamos National Lab. Report, LA-13070-MS.

Farrar, C.R. and Jauregui, D.V. (1998) Comparative study of damage identification algorithms applied to a bridge: I. Experimental, Smart materials and Structures Vol 7, pp 704–719.

Farrar, C.R., Baker, W.E., Bell, T.M., Cone, E.M., Darling, T.W., Duffey, T.A. et al. (1994) Dynamic characterization and damage detection in the I-40 bridge over the Rio Grande, Los Alamos National Laboratory, Report LA-12767-MS.

Sampaio, R.P.C., Maia, N.M.M. and Silva, J.M.M. (1999) Damage detection using the Frequency Response Function Curvature method, Journal of Sound and Vibration Vol 226, pp 1029–1042.

Torrence, C. and Compo, G.P. (1998) A Practical guide to wavelet analysis, Bulletin of the American Meteorological Society Vol 79, pp 61-78.

Yam, L.H., Yan, Y.J. and Jiang, J.S. (2003) Vibration-based damage detection for composite structures using wavelet transform and neural network identification, Composite Structures Vol 60, pp 403-412.

Zhang, Z. and Aktan, A.E. (1998) Application of modal flexibility and its derivatives in structural identification, Research in Nondestructive Evaluation Vol 10, pp 43–61.